CZECH TECHNICAL UNIVERSITY IN PRAGUE

FACULTY OF MECHANICAL ENGINEERING

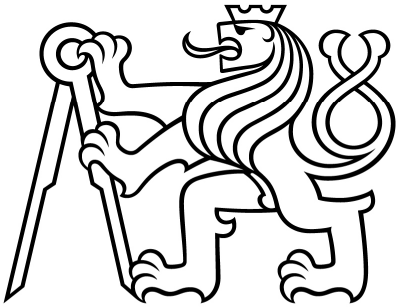

DOCTORAL THESIS STATEMENT

CZECH TECHNICAL UNIVERSITY IN PRAGUE
FACULTY OF MECHANICAL ENGINEERING
DEPARTMENT OF MECHANICS, BIOMECHANICS AND MECHATRONICS

DOCTORAL THESIS STATEMENT

Constitutive Modeling of Human Saphenous Veins under 3D Stress State

Jan Veselý

Doctoral study program: Mechanical Engineering
Study branch: Biomechanics

Supervisor: prof. Ing. Rudolf Žitný, Csc.
Dissertation advisor: Doc. Ing. Lukáš Horný, Ph.D.

Prague May 2017

Disertační práce byla vypracována v prezenční a posléze v kombinované formě doktorského studia na Ústavu Mechaniky, biomechaniky a mechatroniky, Fakulty strojní ČVUT v Praze.

Disertant: Ing. Jan Veselý
Ústav mechaniky, biomechaniky a mechatroniky
Fakulta strojní ČVUT v Praze,
Technická 4, Praha 6, 166 07

Školitel: prof. Ing. Rudolf Žitný, CSc.
Ústav procesní a zpracovatelské techniky
Fakulta strojní ČVUT v Praze
Technická 4, Praha 6, 166 07

Školitel specialista: Doc. Ing. Lukáš Horný, Ph.D.
Ústav mechaniky, biomechaniky a mechatroniky
Fakulta strojní ČVUT v Praze
Technická 4, Praha6, 166 07

Oponenti: ……
……

……
……

……
……

Teze byly rozeslány dne: .....

Obhajoba disertace se koná dne ..... v …… hod. před komisí pro obhajobu disertační práce ve studijním oboru Biomechanika v zasedací místnosti č…. Fakulty strojní ČVUT v Praze, Technická 4, Praha 6.

S disertací je možno se seznámit na oddělení vědy a výzkumu Fakulty strojní ČVUT v Praze, Technická 4, Praha 6.

Předseda oborové rady: prof. RNDr. Matěj Daniel, Ph.D.
Fakulta strojní ČVUT v Praze

Summary

The presented study deals with inflation experiments at free axial extensions of 15 human vena saphena magna which were conducted ex vivo to obtain data suitable for multi-axial constitutive modeling at overloading conditions (pressures up to approximately 15 kPa). Subsequently the data were fitted with a hyperelastic, nonlinear and anisotropic constitutive model based on the theory of the closed thick-walled tube. The material parameters presented here are suitable for use in mechanobiological simulations describing the procedures during intervention or adaptation of the autologous vein wall after bypass surgery.

It was observed that initial highly deformable behavior (up to approximately 2.5 kPa) in the pressure–circumferential stretch response is followed by progressive large strain stiffening. Contrary to that, samples were much stiffer in longitudinal direction, where the observed stretches were in the range 0.98 – 1.03 during the entire pressurization in most cases. The effect of possible residual stress was evaluated in the simulation of the intramural stress distribution with the residual strain (opening angle) prescribed from 0° to 90°. The result suggests that for representative donor the optimal opening angle making the stress distribution through the wall thickness uniform should be expected from 40° to 50°.

The residual strain in the circumferential direction (opening angle) was also quantified by opening angle experiments. Rings of the vein from four donors were radially cut to obtain the opening angle of the tissue. It was found that the average opening angle is 45° ± 18° (mean ± SD). Then, the findings were compared to the simulations of the optimal residual strain (opening angle is homogenizing the stress distribution across the wall thickness). The results suggest that opening angle obtained from experiments is close to the value of opening angle which homogenizes the stress distribution across the wall thickness determined from simulations.

Anotace

Předkládaná práce si dává za cíl charakterizovat mechanické chování materiálu lidské velké skryté žíly, která se velmi často používá jako štěp, při aorto – koronárním bypassu. Tlakovací testy byly provedeny pro 15 dárců skryté žíly ex-vivo, za účelem obdržení experimentálních dat vhodných pro multi-axialní konstitutivní modelovaní (žíly byly tlakovány přibližně do 15 kPa). Následně byla tato data fitována hyperelastickým, nelineárním a anizotropním konstitutivním modelem, který uvažuje žílu jako uzavřenou silnostěnnou válcovou nádobu. Bylo zjištěno, že na počátku tlakování (přibližně do vnitřního tlaku 2,5 kPa) jsou žíly velice poddajné v obvodovém směru, při dalším zvyšování tlaku však žíly výrazně tuhnou. Testy ukázaly, že v podélném směru jsou žíly mnohem tužší, než ve směru obvodovém – streče pozorované v axiálním směru se ve většině případů pohybovaly v rozmezí 0,98 – 1,03.

Na základě simulací byla následně hledána velikost optimální zbytkové deformace v obvodovém směru (tzv. úhel rozevření). Pro úhly rozevření v intervalu 0° - 90°bylo vypočítáno rozložení napětí přes tloušťku stěny. Jako optimální zbytková deformace byla označena ta hodnota, která homogenizuje toto rozložení (hypotéza uniformního rozložení napětí po tloušťce stěny). Bylo zjištěno, že pro reprezentativního dárce se dá očekávat hodnota úhlu rozevření v rozmezí od 40°do 50°.

Zbytková deformace byla také změřena pro 4 dárce. Kroužky žíly byly radiálně rozříznuty a následně byla odečtena hodnota úhlu rozevření. Byla zjištěna průměrná hodnota 45° ± 18° (střední hodnota ± SD). Srovnání se simulacemi ukázalo, že změřená hodnota se velice blíží té, která byla obdržena z provedených výpočetních simulací.

Table of Content

1. Introduction

Coronary artery disease (CAD) is also known as ischemic heart disease (IHD) is a group of diseases that includes atherosclerosis, angina pectoris, myocardial infarction, and sudden cardiac death. It is the most important cause of morbidity and mortality worldwide. In 2013 CAD globally resulted in 8.14 million deaths (16.8%) up from 5.74 million deaths (12%) in 1990 (GBD 2013). Typically, coronary artery disease occurs when part of the smooth, elastic lining inside an artery develops atherosclerosis. It is a condition in which the atherosclerotic plaque consisting of calcium deposits, fatty deposits, and abnormal inflammatory cells builds up inside the artery. It's a complex process. Exactly how atherosclerosis begins or what causes it isn't known, but some theories have been proposed. Many scientists believe plaque begins to form because the inner lining of the artery (intima) becomes damaged. There are main three possible causes of damage to the arterial wall:

- Elevated levels of cholesterol and triglycerides in the blood
- High blood pressure
- Cigarette smoking

Because of the damage, fats, cholesterol, platelets, cellular debris and calcium accumulate over time in the artery wall. These substances may stimulate the cells of the artery wall to produce other substances, resulting in the accumulation of more cells in the innermost layer of the artery wall where the atherosclerotic lesions form. These cells accumulate, and many divide. At the same time, fat builds up within and around these cells. They also form connective tissue. The arterial wall becomes markedly thickened by these accumulating cells and surrounding material. The artery narrows and blood flow is reduced, thus decreasing the oxygen supply. Often a blood clot forms and blocks the artery, stopping the flow of blood. If the oxygen supply to the heart muscle is reduced, a heart attack can occur. Treatment of coronary artery disease starts with life changes, such as eating a healthy diet, stop smoking and exercising. In more complicated cases, medications which can slow or even reverse the effects of atherosclerosis.

Sometimes more aggressive treatment is needed to treat CAD surgically. Angioplasty is an endovascular procedure to widen narrowed or obstructed arteries or veins, typically to treat arterial atherosclerosis. An empty, collapsed balloon, known as a balloon catheter, is passed over a wire into the narrowed locations and then inflated to a fixed size. The balloon forces

expansion of the stenosis (narrowing) within the vessel and the surrounding muscular wall, opening up the blood vessel for improved flow, and the balloon is then deflated and withdrawn. A stent may also be placed in the blocked area. The stent is inserted at the same time as the balloon catheter. It expands when the balloon is blown up. The stent is left in place to help keep the artery open. Percutaneous coronary intervention (PCI), commonly known as coronary angioplasty is a procedure to treat the stenotic (narrowed) coronary arteries of the heart, Fig. 1.

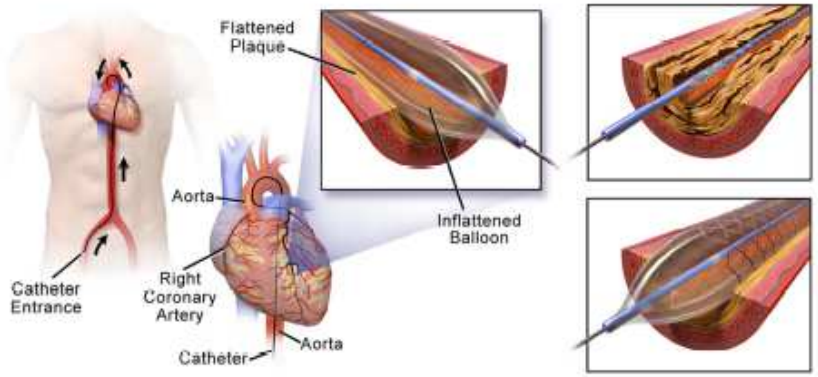

Fig. 1 The procedure of PCI in stenotic coronary artery. Left – balloon angioplasty. Right – stent insertion. Adopted and modified from https://en.wikipedia.org/wiki/File:BalloonTipped_Catheter.png.

The coronary artery bypass graft surgery (CABG) is the procedure to treat coronary artery disease in its last stages, Fig. 2. The place of blockage in the artery is overbridged by a vessel from another part of patient's body or a tube made of synthetic fabric. This allows blood to flow around the blocked or narrowed artery. Although arterial grafts are preferred as bypass conduits because of their better patency rates, their use is limited because of the length and number of available segments. Therefore, the saphenous vein (SV) is most often used as an arterial bypass graft in the coronary circulation (Athanasiou et al., 2011). However, its patency is relatively low (less than 50% in 10 years) compared with the patency rate of arterial grafts (Fitzgibbon et al., 1978; Fitzgibbon et al., 1996). Saphenous veins' properties are, however, optimized for a mechanical environment very different from arterial conditions. Immediately after the surgery, remodeling processes are triggered and the vein adapts to the elevated blood pressure, flow rate and

oscillatory wall shear stress. As an undesirable effect of the changed conditions, the patency of the graft may be substantially compromised by an intimal hyperplasia or thrombosis (Fitzgibbon et al., 1996; Hwang et al. 2012).

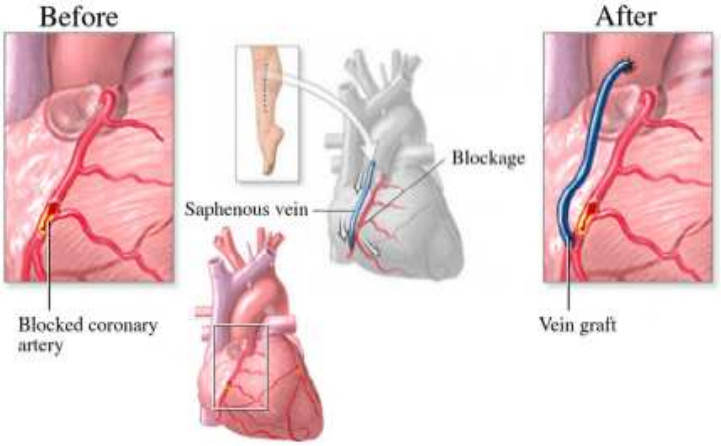

Fig. 2 Coronary artery bypass graft surgery. The place of blockage is overbridged by the venous graft. Adopted from http://www.adamimages.com/.

Much work is now being done to deepen our knowledge of the mechanobiology of graft remodeling, but this process is still not completely understood (Tran-Son-Tay et al., 2008; Hwang et al., 2012; Hwang et al., 2013; Sassani et al., 2013). The adaptation to the changed conditions leads not only to a change in the diameter and thickness of the graft wall, but also to a changed internal structure and thus a change in the constitutive equation expressing the mutual relation between stress and strain (Hwang et al., 2012). Moreover, not only the wall shear stress, but also changed intramural stresses initiate the remodeling (Eberth et al., 2011; Humphrey et al., 2009). Besides the overall effect of elevated blood pressure, there are local stress concentrations in artery-graft anastomoses caused either by the specific geometry of the anastomosis or by a general compliance mismatch (Ballyk et al., 1998; Cacho et al., 2007).

In contrast to the work done on arteries, there have been only a few papers describing the multi-axial mechanical response of veins within the framework of nonlinear elasticity (Desch and Weizsäcker, 2007; Cacho et al., 2007; McGilvray et al., 2010; Sokolis, 2013; Zhao et al., 2007). Very little

experimental (mechanical) data are, however, available on graft vessels. The bypass graft for a coronary artery can be a healthy artery taken from the arm or chest, or a vein taken from the leg. Probably, the most comprehensive study of mechanical properties of saphenous veins has been provided by Donovan et al. (1990), who performed uniaxial tensile tests in two orthogonal directions of 45 human SVs, and who described their mechanical properties in terms of material constants. More recently, valuable pressure–diameter data have been published by Stooker et al. (2003), comparing human SVs from the upper and lower leg. However, data reported here are expressed as dimensionless values and actual dimensions are not provided, which makes it more difficult to recover the material parameters. Wesly et al. (1975) also reported pressure–diameter relationships, but without arriving at the constitutive equations. The pressurization tests with SVs were also performed by Zhao et al. (2007). The exponential strain energy function proposed by Fung (1993) was used in this study, however, veins were modeled as inflated thin-walled tube which is unsuitable model with respect to the wall thickness, diameter and existence of residual stresses in the wall of the veins.

For over a century it has been considered that blood vessels are stress free when they are removed from the body (Chuong and Fung, 1983; Weizsacker and Pinto, 1988; Holzapfel et al., 2007). It was Fung (1983) and Vaishnav (Vaishnav and Vossoughi, 1983) and their colleagues who initiated the study of residual stress and deformation in arteries. This was followed by the work of Choung and Fung (1986) and Takamizawa and Hayashi (1987), who documented the important implications of the influence of residual stress in arteries. The existence of residual stress is manifested in the springing open of an arterial ring when it is cut in the radial direction (so called opening angle measurement). This opening relieves the residual stress, the circumferential component of which is compressive on the inner part of the ring and tensile on the outer part (Holzapfel et al. 2007), Fig. 3.

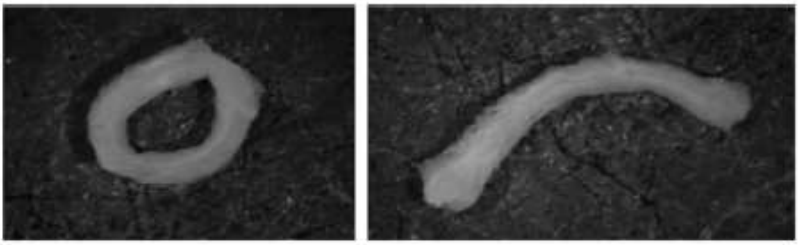

Fig. 3 Ring of saphenous vein before and after radial cut shows the effect of residual stresses in the wall. Adopted from Zhao et al. (2007).

Several authors have shown that although residual stresses are small compared with in vivo wall stresses they have a strong influence on the in vivo stress distribution (Holzapfel et al., 2000; Takamizava and Hayashi, 1987; Takamizava and Hayashi, 1988). In particular, the residual stresses seem to have the effect of homogenizing the circumferential stress within each layer (uniform stress or strain hypothesis) in the physiological load state (Holzapfel et al., 2000; Takamizava and Hayashi, 1987; Chuong and Fung, 1986). Without residual stresses relatively large stress gradients would occur in the blood vessel wall. Although, there are numerous papers about residual strain quantification within the arterial wall, veins received less attention. Huang and Yen (1998) were able to measure residual strain (opening angle) for human pulmonary vein segments with diameter comparable to saphenous veins (opening angle from 90° to 130°). More recently, Zhao et al. (2007) examined the biomechanical properties of human saphenous veins at supraphysiologic pressures using the distension experiment and were able to measure the zerostress state of vein tissue by radially cutting open their specimens. They observed the residual opening angle around 120°. Since the residual strain has significant influence on the stress distribution within the blood vessel wall, the measurement of opening angle was included into this study.

In last decade, the development of numerical computation methods enables to perform simulations to model different phenomena in human body including bypass graft surgery. There are numerous studies available in the literature focusing on anastomotic flow dynamics, see, e.g., Migliavacca and Dubini (2005); Loth et al. (2008). Surprisingly, however, there are only very few studies available dealing with the related solid mechanics (Ballyk et al., 1998; Gu et al., 2006; Leuprecht et al., 2002), and the fluid–structure interaction (Leuprecht et al., 2002; Hofer et al., 1996) of bypass grafts. Although, the simulation methods are powerful tools which give us valuable information, the results are dramatically influenced by the quality of experimentally-determined mechanical properties of the tissue involved in these simulations (Cacho et al., 2007).

The main goal of this study is to find constitutive equations for the multi-axial state of stress suitable for describing the passive nonlinear anisotropic mechanical behavior of human vena saphena magna. Our approach is based on the strain energy density function suggested by Holzapfel et al. (2000). Experimental data were obtained in ex vivo inflation tests (with free axial extension) conducted with samples obtained from fifteen donors.

2. Aim of the Study

Although the saphenous veins are most often used as an arterial bypass graft in the coronary circulation, there is a lack of experimental data and related constitutive modeling in the literature. Therefore, the main goal of this study is to **characterize mechanical response of saphenous vein under 3D stress state and offer constitutive parameters which could be used in the computational simulation of these grafts.**

Nowadays we also know that for instance arteries exhibit residual stresses. Artery rings cut radially spring open to release these stresses. These residual stresses help to tone down the stress gradient across the blood vessel thickness (the uniform stress hypothesis) and prevent the inner surface from overloading. The second aim of this work was to **verify the uniform stress hypothesis for human saphenous veins**. To the best of author's knowledge, such study cannot be found in the literature.

Partial targets:

- Derive the mathematical model and proposal of regression procedure
- Design and adjustment of inflation-extension test set-up
- Proposal and adjustment of the procedure for residual strain measurement

3. Material and Methods

3.1 Material

Two types of experiments were performed during this study (inflation-extension test and opening angle measurement) with samples of great human saphenous vein. **Samples for inflation-extension tests** were collected either during coronary-artery bypass surgery conducted at the General University Hospital in Prague (obtained with informed consent) or during autopsies conducted at the Department of Forensic Medicine of the Third Faculty of Medicine of Charles University in Prague within 24 hours after death. The experimental protocol was approved by the institutional Ethical Committees. Collected veins were placed in the physiological solution and tested in less than three hours after excision. **Specimens for residual strain measurement** were excised during autopsies conducted at the Department of Forensic Medicine of the Third Faculty of Medicine of Charles University in Prague within 24 hours after death. The usage of samples for tests was also approved by the Ethics Committee. Specimens were placed in the physiological solution and tested in five hours after excision. Only the veins with no substantial deviation from circular cylindrical geometry were included into the study. Prior to the mechanical testing, two rings were cut out from the tissue at both ends, and the mean reference dimensions of the samples (external radius, thickness) were determined by means of image analysis of digital photographs (Nis-Elements, Nikon Instruments Inc., NY, USA).

3.2 Inflation-extension Test

Each specimen was marked with a black liquid eye-liner, cannulated at one end and hung vertically in the experimental setup (Fig. 4). The experimental protocol consisted of four pre-cycles to stabilize the mechanical response (preconditioning), and a fifth cycle was used in the data analysis. Pressurization was performed in the range from 0 up to $\approx$15 kPa using a motorized syringe (Standa Ltd, Vilnius, Lithuania). The intraluminal pressure was monitored by pressure transducer (Cressto s.r.o, Czech Republic). The deformed geometry was recorded by a CCD camera (Dantec Dynamics, Skovlunde, Denmark). In the data post processing, changes in the length between the black marks (Fig. 4) and average changes in the silhouette (also between the marks to avoid end effects) were determined by the edge detection algorithm in Matlab (MathWorks, MA, USA). They were used to compute axial stretch ratio λ_z and circumferential stretch ratio at the outer radius $\lambda_\theta(r_o)$. The experiments were performed at room temperature (22°C).

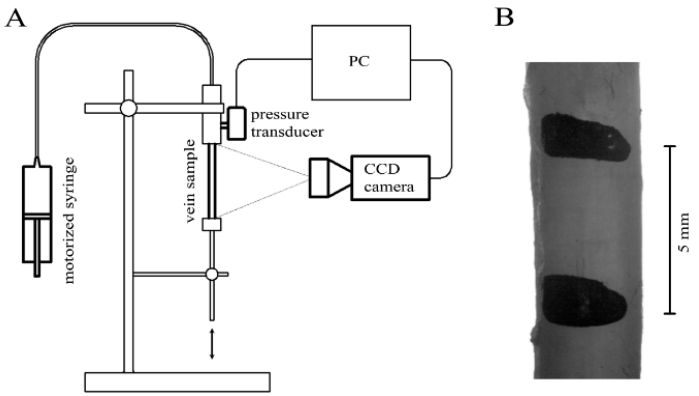

Fig. 4 Experimental inflation-extension test set-up (panel A), and a picture of the sample taken with a CCD camera (panel B). The black marks were used to identify the longitudinal deformation of the vein.

3.3 Opening Angle Measurement

The methodology of the opening angle measurement was finally created after several unsuccessful efforts. Four samples of healthy human saphenous veins were excised during autopsy and surrounding connective tissue and fat were removed. Three rings were cut from each sample and placed in the physiological solution. The rings were then cut radially and left to release the residual stresses for 30 minutes to allow viscoelastic creep to take place (Fung, 1993). The opening angle was measured from photographs (Nis-Elements, Nikon Instruments Inc., NY, USA)., Fig. 5. The final value of opening angle for each donor was obtained as average from all three cut rings.

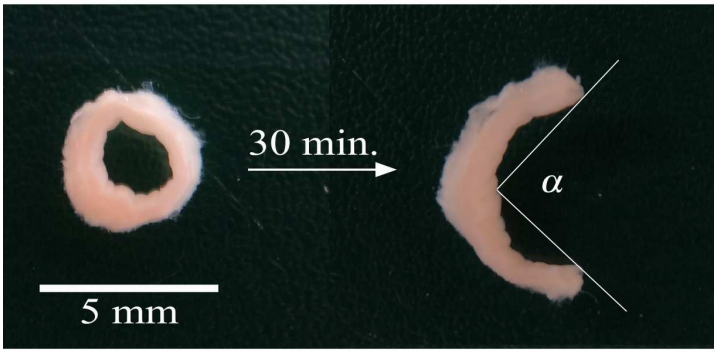

Fig. 5 Ring of saphenous vein before radial cut and after 30 minutes with released residual stresses. Adopted from Veselý et al. 2015b

3.4 Theoretical Framework

Kinematics

The vein was considered to be a homogeneous, incompressible cylindrical thick-walled tube. The kinematics of the experiment was modeled as simultaneous inflation and extension, in which the material particle located in the reference (stress free) configuration in the position $\boldsymbol{X} = (R, \Theta, Z)$ is mapped by the deformation into the position $\boldsymbol{x} = (r, \theta, z)$ in the current configuration, according to equation (1).

$$r = r(R) \quad \theta = \Theta \quad z = \lambda_z Z \tag{1}$$

The situation is depicted in Fig. 6. Here R_o and R_i respectively denote the outer and inner radius in the reference configuration ($R_i \leq R \leq R_o$) and r_o and r_i in the deformed configuration ($r_i \leq r \leq r_o$). By analogy, H and h denote thickness of the tube and L ($0 \leq Z \leq L$) and l ($0 \leq z \leq l$) denote its length measured between the marks.

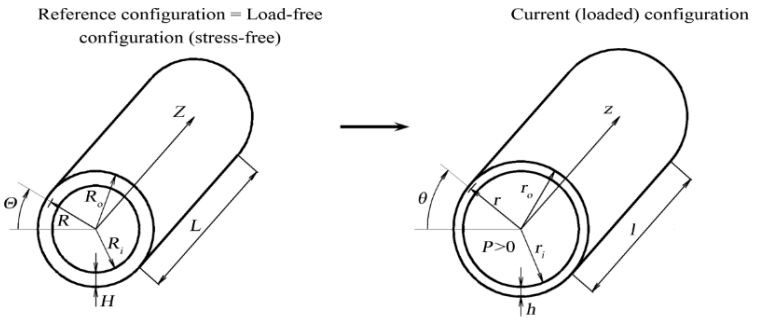

Fig. 6. Kinematics of the deformation of the vein wall. The stress-free configuration (assumed to be the same as the load-free configuration) and the deformed current (loaded) configuration are depicted.

The deformation gradient $\mathbf{F} = \partial \mathbf{x}/\partial \boldsymbol{X}$ is then described by equation (2). Here the longitudinal stretch ratio was considered to be uniform. The assumption of incompressibility is expressed via the kinematical constraint $\det\mathbf{F} = 1$, which allows us to write λ_r also as $\lambda_r = 1/(\lambda_\theta \lambda_z)$.

$$\mathbf{F} = \begin{pmatrix} \lambda_r(r) & 0 & 0 \\ 0 & \lambda_\theta(r) & 0 \\ 0 & 0 & \lambda_z \end{pmatrix} = \begin{pmatrix} \dfrac{\partial r}{\partial R} & 0 & 0 \\ 0 & \dfrac{r}{R} & 0 \\ 0 & 0 & \dfrac{l}{L} \end{pmatrix} \tag{2}$$

It is useful to express the incompressibility condition by means of the radius and the length: $\pi L(R_o^2 - R_i^2) = \pi l(r_o^2 - r_i^2)$. This was used to compute the inner radius during the deformation. From here, substituting R_i by R and r_i by r, we also arrive at $R = R(r)$ required in $\lambda_\theta(r)$ expression.

Constitutive model

The material of *vena saphena magna* was considered to be an anisotropic hyperelastic continuum characterized by the strain energy density function W proposed by Holzapfel et al. (2000). The anisotropy arises from two families of preferred directions (interpreted as the orientation of the collagen fibers)

symmetrically disposed with respect to the circumferential axis. This is expressed mathematically in equation (3).

$$W = W_{isotropic} + W_{anisotropic} = \frac{\mu}{2}(I_1 - 3) + \frac{k_1}{2k_2}\sum_{i=4,6}\left\{\exp\left[k_2\left(I_i - 1\right)^2\right] - 1\right\} \qquad (3)$$

This expression consists of a neo-Hooke term with a stress-like material parameter $\mu > 0$. I_1 is the first invariant of the right Cauchy-Green strain tensor **C**, $\mathbf{C} = \mathbf{F}^T\mathbf{F}$. The specific mathematical expression of I_1 is in (4). The neo-Hooke term represents the energy stored in the process of a deformation in the whole non-collagenous matter (elastin, smooth muscle cells, proteoglycans) of the vein wall.

$$I_1 = \lambda_r^2 + \lambda_\theta^2 + \lambda_z^2 \qquad (4)$$

Significant large strain stiffening of the soft tissues is ascribed to the collagen fibrils, and is modeled in (3) by an exponential function with stress-like parameter $k_1 > 0$ and dimensionless $k_2 > 0$. I_4 and I_6 are additional strain invariants arising from the existence of two preferred directions. In our case (no shear strain, and collagen fibrils creating helixes in the surfaces characterized by R = constant), they can be expressed by equation (5). Here β denotes the inclination from the circumferential axis (the second helix runs with angle $-\beta$, but due to the symmetry only equation (5) is necessary).

$$I_4 = I_6 = \lambda_\theta^2 \cos^2\beta + \lambda_z^2 \sin^2\beta \qquad (5)$$

Finally, the constitutive equation for an incompressible hyperelastic material can be written in the form of (6). Here **σ** denotes the Cauchy stress tensor and p is an undetermined multiplier induced by incompressibility constraint.

$$\boldsymbol{\sigma} = 2\mathbf{F}\frac{\partial W}{\partial \mathbf{C}}\mathbf{F}^T - \mathbf{I}p \qquad (6)$$

Thick-walled tube model

Let us denote as $\hat{W}$ the strain energy density function (3) with eliminated explicit dependence on λ_r by substituting $\lambda_r = 1/(\lambda_\theta\lambda_z)$. Considering the boundary conditions $\sigma_{rr}(r_i) = -P$ and $\sigma_{rr}(r_o) = 0$, the equilibrium equations in

the radial and axial direction have the form (7) and (8), respectively. Here P denotes internal pressure and F_{red} is the reduced axial (prestretching) force acting on the closed end of the tube additionally to the force generated by the pressure acting on the end (Horny et al., 2014a; Horny et al., 2014b; Matsumuto and Hayashi, 1996).

$$P = \int_{r_i}^{r_o} \lambda_\theta \frac{\partial \hat{W}}{\partial \lambda_\theta} \frac{dr}{r} \tag{7}$$

$$F_{red} = \pi \int_{r_i}^{r_o} \left(2\lambda_z \frac{\partial \hat{W}}{\partial \lambda_z} - \lambda_\theta \frac{\partial \hat{W}}{\partial \lambda_\theta} \right) r dr \tag{8}$$

Determination of the material parameters

The material parameters (μ, k_1, k_2, β) of the constitutive model were determined by fitting model predictions based on (7) and (8) to the experimental data. The objective function Q (9) was minimized in Maple (Maplesoft, Waterloo, Canada). P^{mod} and P^{exp} in (9) denote the internal pressure predicted by (7) and measured experimentally, respectively. The same denotation applies for axial force F_{red}. Neglecting the small weight of the tube's lower plug ($\approx$5g), $F_{red}{}^{exp}$ was considered to be 0. w_p and w_F are weight factors. n is the number of observation points.

$$Q = \sum_{j=1}^{n} \left\{ \left[w_p \left(P_j^{mod} - P_j^{exp} \right) \right]^2 + \left[w_F \left(F_{redj}^{mod} - F_{redj}^{exp} \right) \right]^2 \right\} \tag{9}$$

Opening angle estimation

To provide qualified estimate of how large the residual strain in the venous wall could be, we computed the intramural distribution of the circumferential and axial stress in one representative case (donor M60a) for opening angles $\alpha = 0°$, $\alpha = 10°$, $\alpha = 20°$, $\alpha = 30°$, $\alpha = 40°$ and $\alpha = 50°$. The method is based on the assumption that the opened up geometry is modeled as a circular sector, as explained in detail for instance in Chuong and Fung (1986), Rachev and Greenwald (2002), Holzapfel et al. (2000), Horny et al. (2014a,b). Adopted approach modifies Eq. (1b) and incompressibility condition mentioned above to the form (10a) and (10b), respectively. Here ρ_o and ρ_i denote outer and inner radius of opened up circular sector.

$$\theta = \frac{\pi}{\pi - \alpha}\Theta \quad \pi l\left(r_o^2 - r_i^2\right) = \left(\pi - \alpha\right) L\left(\rho_o^2 - \rho_i^2\right) \tag{10}$$

Values of the intramural stress gradient for P = 2.3 kPa (representative venous pressure) and P = 13.3 kPa (representative arterial pressure) were computed according equation (11). We assumed that the optimal opening angle homogenizes the stress distribution across the wall thickness ($SR_k^P = 1$).

$$SR_k^P = \frac{\sigma_{kk}\left(r_i\right)}{\sigma_{kk}\left(r_o\right)} \qquad for\, k = \theta, z \quad and \quad P = 2.3kPa, 13.3kPa \tag{11}$$

4. Results

The data collected in the experiments are summarized in Table 1. Eleven samples of human saphenous vein were collected during surgery (mean ± SD; age 55 ± 15; 7 male and 4 female; 3 donors with varicose disease) and four in autopsy (age 65 ± 5; 3 male and 1 female; one with varicose disease). Fig. 7 shows the loading part of the fifth inflation-extension cycle to which the constitutive models were fitted. Model predictions were obtained by substituting the estimated parameters into the system (7) and (8), and are depicted by continuous curves (donors with varicose disease are in red).

The models predict satisfactorily the experimental pressure-stretch data (Fig. 7 upper panel). However, the predicted axial stretch, shown in Fig. 7 (bottom panel), corresponds to the experiments only to a limited extent. Computed intramural distributions of the circumferential and axial stress for donor M60a for P = 2.3 kPa (representative venous pressure) and P = 13.3 kPa (representative arterial pressure) are depicted in Fig. 8 with indicated numerical values of the intramural stress gradient (SR_k^P). The measured opening angles for each donor (two male and two female; age 62±5 years) and mean value from all measurements are displayed in Fig. 9.

Table 1. Age and sex of the donors (F stands for female and M for male), obtained material parameters (μ, k_1, k_2, β) for each sample of vein.

Donor	Age [years]	Sex	R_o [mm]	H [mm]	Material parameters				Pathology
					μ [kPa]	k_1 [kPa]	k_2 [-]	β [°]	
CABG									
a	63	M	2.89	0.83	5.5	4.0	61.7	40.3	-
	66	F	2.12	0.49	28.4	8.4	122.1	39.3	varicose
	27	F	2.32	0.88	4.0	1.5	18.2	43.0	varicose
	42	F	2.78	0.80	5.7	1.4	13.5	43.1	varicose
	69	M	1.14	0.59	4.2	3.0	10.8	44.1	-
b	63	M	2.05	0.76	5.6	4.5	13.6	42.7	-
a	60	M	1.80	0.53	9.9	5.9	62.2	39.8	-
	76	M	1.98	0.57	7.0	19.3	48.2	36.5	-
	50	M	2.33	0.57	30.7	30.3	330	38.4	-
b	60	M	1.92	0.47	13.7	9.3	85.5	38.2	-
	49	F	1.86	0.39	14.1	4.2	43.2	41.2	-
Mean	55	-	2.11	0.62	11.7	8.3	73.6	40.6	-
SD	15	-	0.48	0.16	9.1	8.4	87.5	2.3	-
Autopsy									
	72	F	1.78	0.71	3.1	2.3	8.8	42.6	-
c	60	M	0.92	0.28	9.5	5.0	53.5	41.5	-
d	60	M	2.14	0.42	4.4	1.4	50.5	40.4	-
	68	M	1.80	0.48	4.2	1.0	13.1	41.9	varicose
Mean	65	-	1.66	0.47	5.3	2.5	31.5	41.6	-
SD	5	-	0.52	0.18	2.5	1.6	20.6	0.8	-

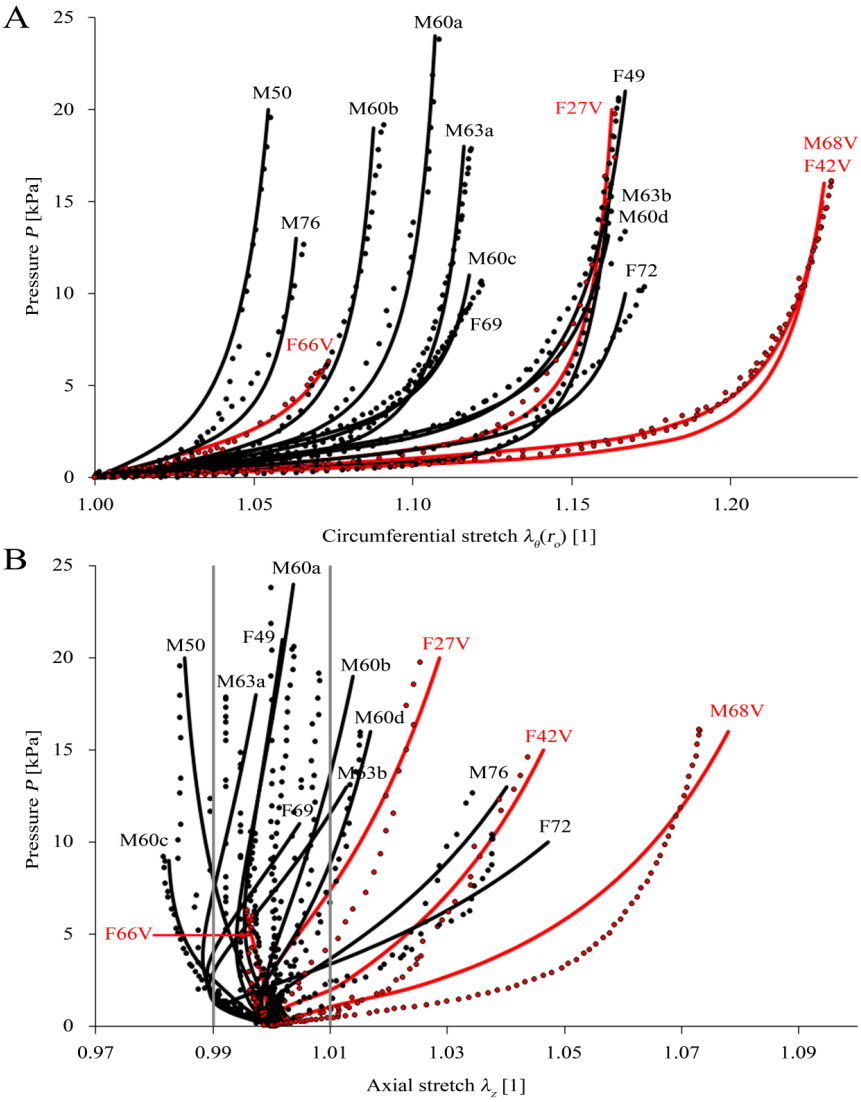

Fig. 7 The resulting pressure-circumferential stretch at the outer radius (panel A) and pressure-axial stretch (panel B) dependences. The experimental data (dotted curves) are compared with data predicted by the constitutive model (solid curves). The donors with varicose disease are in red. The interval in

axial stretch from 0.99 to 1.01 in panel B identified by gray lines represents bounds of uncertainty caused by resolution of digital cameras.

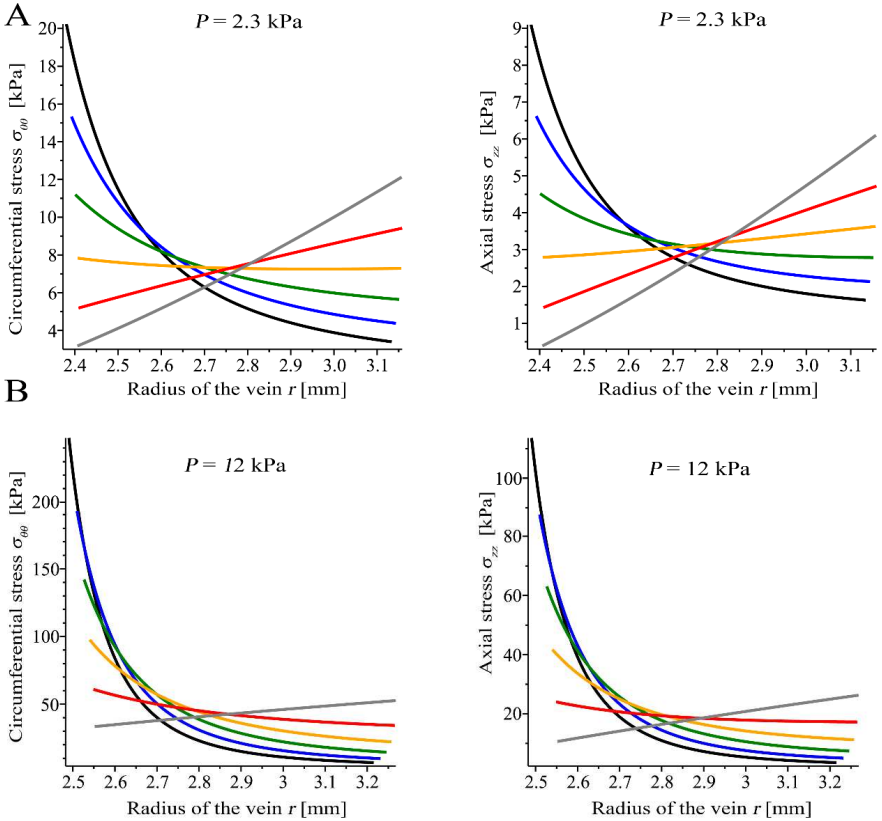

C

	$\alpha = 0°$	$\alpha = 10°$	$\alpha = 20°$	$\alpha = 30°$	$\alpha = 40°$	$\alpha = 50°$
$SR_{\theta}^{2.3kPa}$	5.95	3.50	1.98	1.07	0.55	0.26
$SR_{z}^{2.3kPa}$	5.59	3.11	1.62	0.77	0.30	0.06
SR_{θ}^{12kPa}	36.39	19.75	9.81	4.41	1.77	0.63
SR_{z}^{12kPa}	32.36	17.41	8.51	3.71	1.39	0.40

Fig. 8 The simulation of the influence of opening angle α for donor M60a. The circumferential and axial stress gradient through the vein wall for transmural pressure 2.3 kPa (panel A) and for 13.3 kPa (panel B). Panel C displays stress gradients through the wall thickness.

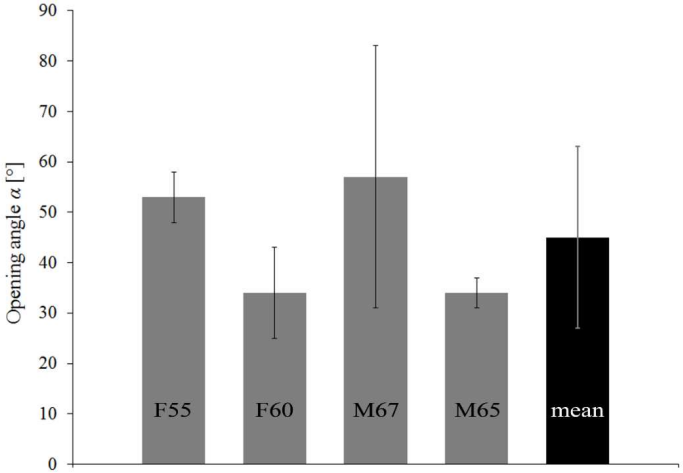

Fig. 9 Obtained values of the opening angles for each donor (grey) and the average from all measurements (black) with related standard deviations. Adopted and modified from Veselý et al. 2015b.

5. Discussion

In our study, overloading inflation-extension tests were performed with 15 human saphenous veins. The experiments were conducted with free axial extension of the tubes without axial pre-stretch. This approach was chosen in order to simulate conditions after implantation of the graft in arterial system. The experimental data were fitted by the hyperelastic nonlinear anisotropic constitutive model proposed by Holzapfel et al. (2000). Only the passive mechanical response was modelled.

Fig. 7 shows that veins under simultaneous inflation and extension exhibit significantly smaller deformations in axial direction than in circumferential direction. It may be a consequence of approximately two-times smaller stresses in axial than in circumferential direction, as it is shown in Fig. 8 for donor M60a ($\alpha = 0°$, black curves). This finding is in agreement with results of Wesly et al. (1975), who studied the pressure-strain relationship of dog jugular and human saphenous veins. Specifically, in our study measured axial stretches are generally in the range from 0.98 to 1.03. For samples M50, M63a, F49, M60a, F69, F66V, M60d and M63b, the range of axial deformation during the entire pressurization period was not higher than

approx. 1%. This small deformation is, however, determined with relatively high measurement uncertainty. In the worst case, the resolution of the digital images was 19 pixels/mm (M76). In this case, the reference distance of the longitudinal marks was 104 pixels. Thus to obtain axial extension of 1%, it would be necessary to find marks at a distance of 105.04 pixels. This is a change of 1 pixel. Due to this fact axial stretches in the interval from 0.99 to 1.01 are affected by experimental uncertainty which is in Fig. 7 highlighted by gray lines. In this case, we decided to present in Fig. 7 predictions of the simulation based on (7) and (8) with substituted (3) in which $\lambda_\theta(r_o)$ and λ_z were also based on the model rather than solely predicting P at the experimentally obtained stretches, which may be affected by measurement error. This approach, however, gives somewhat different λ_z than was measured experimentally.

Four donors with diagnosed varicose disease were included in this study in order to reveal differences in mechanical response in comparison with healthy donors. However, we were able to obtain only four samples which is a small number for statistical evaluation and these samples do not appear to behave differently. Finally, we preserved them in the study, because obtained material parameters could be used by other authors.

In our study, it was assumed that veins are in stress-free configuration in their cylindrical geometry. This is the most important limitation of our study, since it is well known that for instance arteries exhibit residual stresses. Artery rings cut radially spring open to release these stresses; this is the so-called opening angle method (Chuong and Fung 1986, Rachev and Greenwald 2002, Holzapfel et al., 2000). Zhao et al. (2007) examined the biomechanical properties of human saphenous veins at supra-physiologic pressures using the distension experiment and were able to measure the zero-stress state of vein tissue by radially cutting open their specimens. They observed the residual opening angle around 120°. Similar results (opening angle from 90° to 130°) were obtained by Huang and Yen (1998) for human pulmonary vein segments with diameter comparable to saphenous veins. We also tried to measure the residual strain by the opening angle, but it was impossible with our current technical equipment. The vein walls were so compliant that they collapsed and we could not distinguish between forces imposed by handling and forces induced by the releasing residual stress.

However, to provide at least some qualified estimate of how large the residual stress in the venous wall could be, the intramural distribution of the circumferential and axial stress in one representative case (donor M60a) was computed for opening angles $\alpha = 0°$, $\alpha = 10°$, $\alpha = 20°$, $\alpha = 30°$, $\alpha = 40°$ and $\alpha = 50°$. The computations were provided for pressure P = 2.3 kPa

(representative venous pressure) and for P = 13.3 kPa (representative arterial pressure), which is close to the pressure in great saphenous vein in standing position (approx. 12 kPa) measured by Pollack and Wood (1949) and Neglén and Raju (2000). The results (Fig. 8) suggest that the optimal opening angle (homogenizing the stress distribution across the wall thickness – uniform stress or strain hypothesis; Chuong and Fung, 1986; Takamizawa and Hayashi, 1987) could be expected about 40°. Our results of the opening angle simulations showed that we should anticipate value higher than 0°. However, one can find higher values in observations of Zhao et al. (2007). It is clear that the uniform stress or strain hypothesis for saphenous veins should be addressed in future research and proven experimentally. The results also indicate that under arterial conditions the inner radius of the vein wall could be highly overloaded. This is consistent with the development of intimal hyperplasia after a graft surgery.

To the best of our knowledge, this is the first study witch presents a comprehensive set of material parameters for human saphenous veins modeled as the thick wall tube suitable for describing multi-axial stress states. They can be helpful as input in numerical simulations of the remodeling and adaptation processes triggered after bypass surgery involving autologous vein grafts (Hwang et al., 2012, 2013; Sassani et al., 2013).

After a several unsuccessful efforts, the opening angle of human great saphenous vein was experimentally obtained for four donors. The rings of the vein samples were cut radially and left to release the residual stresses for 30 minutes as it is described for example in Zhao et al. (2007). The observed opening angle suggest that the vein wall is in compression in the no-load state and at the low-pressure range. Thus, the compressed inner wall may be better protected against endothelium damage from high pressure than an uncompressed inner wall. These protection mechanisms could be important when high pressures are reached, e.g. after the saphenous vein is inserted into the coronary circulation during CABG.

The experiments showed no significant differences between donors and the mean value of opening angle $\bar{\alpha}$ = 45°±18° (mean ± SD) for all measurements (Fig. 9). As it was mentioned above, Zhao et al. (2007) observed the opening angle for human saphenous vein around 120° and similar results (opening angle from 90° to 130°) were obtained by Huang and Yen (1998) for human pulmonary veins. Our results showed lower values in all twelve measurements. The differences could be caused by variability between donors included into study. However, we can observe agreement in the values of opening angle, comparing the residual strain measurement with the results obtained from simulations described above (the uniform stress

hypothesis was adopted in order to obtain opening angle which homogenizes the stress distribution across the vein wall). For the representative sample from the inflation-extension tests (donor M60a), the homogenizing opening angle could be expected in the interval 40° - 50°, Fig. 8. These results suggest that the uniform stress hypothesis could be valid not only for arteries but also for the veins. However, this hypothesis should be addressed in future research because in this study, the inflation-extension tests and opening angle measurements were provided for different donors. Future research should also answer the question if the residual strain (opening angle) would be changed after implantation of the graft into arterial conditions and its remodeling. The influence of longitudinal residual strain should be also verified because it plays important role in artery biomechanics (Horny et al., 2012).

References

Athanasiou T., Saso S., Rao C., Vecht J., Grapsa J., Dunning J., Lemma M., Casula R., 2011. Radial artery versus saphenous vein conduits for coronary artery bypass surgery: forty years of competition—which conduit offers better patency? A systematic review and meta-analysis. Eur J Cardiothorac Surg 40:208–220

Ballyk, P.D., Walsh, C., Butany, J., Ojha, M., 1998. Compliance mismatch may promote graft-artery intimal hyperplasia by altering suture-line stresses. Journal of Biomechanics 31, 229-237.

Cacho, F., Doblaré, M., Holzapfel, G.A., 2007. A procedure to simulate coronary artery bypass graft surgery. Medical and Biological Engineering and Computing 45, 819-827.

Canver, C.C., 1995. Conduit options in coronary artery bypass surgery. Chest 108, 1150-1155.

Chuong, C.J., Fung, Y.C., 1986. On residual stresses in arteries. Journal of Biomechanical Engineering 108, 189-192.

Desch, G. W. Weizsäcker, H. W., 2007. A model for passive elastic properties of rat vena cava. Journal of Biomechanics 40, 3130-3145.

Donovan, D.L., Schmidt, S.P., Townshend, S.P., Njus, G.O., Sharp, W.V., 1990. Material and structural characterization of human saphenous vein. Journal of Vascular Surgery 12, 531-537.

Eberth, J. F. Cardamone, L., Humphrey, J. D., 2011. Evolving biaxial mechanical properties of mouse carotid arteries in hypertension. Journal of Biomechanics 44, 2532-2537.

Fitzgibbon, G.M., Burton, J.R., and Leach, A. J., 1978. Coronary bypass graft fate; Angiographic grading of 1400 consecutive grafts early after operation and of 1132 after one year. Circulation 57, 1070–1074.

FitzGibbon, G. M., Kafka, H. P., Leach, A. J., Keon, W. J., Hooper, G. D., Burton, J. R., 1996. Coronary bypass graft fate and patient outcome: Angiographic follow-up of 5,065 grafts related to survival and reoperation in 1,388 patients during 25 years. Journal of the American College of Cardiology 28, 616-626.

Holzapfel, G.A., Gasser, T.C., Ogden, R.W., 2000. A new constitutive framework for arterial wall mechanics and a comparative study of material models. Journal of Elasticity 61, 1-48.

Holzapfel, G. A., 2006. Determination of material models for arterial walls from uniaxial extension tests and histological structure. Journal of Theoretical Biology 238, 290-302.

Horný, L., Netušil, M., Voňavková, T., 2014a. Axial prestretch and circumferential distensibility in biomechanics of abdominal aorta. Biomechanics and Modeling in Mechanobiology 13, 783-799.

Horny, L., Netusil, M., Daniel, M., 2014b. Limiting extensibility constitutive model with distributed fibre orientations and ageing of abdominal aorta. Journal of the Mechanical Behavior of Biomedical Materials 38, 39-51.

Huang, W., Yen, R.T., 1998. Zero-stress states of human pulmonary arteries and veins. Journal of Applied Physiology 85, 867-873.

Humphrey, J. D., Eberth, J. F., Dye, W. W., Gleason, R. L., 2009. Fundamental role of axial stress in compensatory adaptations by arteries. Journal of Biomechanics 42, 1-8.

Hwang, M., Berceli, S. A., Garbey, M., Kim, N. H., Tran-Son-Tay, R., 2012. The dynamics of vein graft remodeling induced by hemodynamic forces: A mathematical model. Biomechanics and Modeling in Mechanobiology, 11, 411-423.

Hwang, M., Garbey, M., Berceli, S. A., Wu, R., Jiang, Z., Tran-Son-Tay, R., 2013. Rule-based model of vein graft remodeling. PLoS ONE 8, e57822.

Institute for Health Metrics and Evaluation. GBD 2013 Protocol: global burden of diseases, injuries, and risk factors. 2013. http://www.healthdata.org/gbd/about/protocol (accessed Nov 3, 2014).

Matsumoto, T., Hayashi, K., 1996. Stress and strain distribution in hypertensive and normotensive rat aorta considering residual strain. Journal of Biomechanical Engineering 118, 62-71.

McGilvray, K. C., Sarkar, R., Nguyen, K., Puttlitz, C. M., 2010. A biomechanical analysis of venous tissue in its normal and post-phlebitic conditions. Journal of Biomechanics 43, 2941-2947.

Neglén, P., Raju, S., 2000. Differences in pressures of the popliteal, long saphenous, and dorsal foot veins. Journal of Vascular Surgery 32, 894-901.

Perera, G.B., Mueller, M.P., Kubaska, S.M., Wilson, S.E., Lawrence, P.F., Fujitani, R.M., 2004. Superiority of Autogenous Arteriovenous Hemodialysis Access: Maintenance of Function with Fewer Secondary Interventions. Annals of Vascular Surgery 18, 66-73.

Pollack, A.A., Wood, E.H., 1949. Venous pressure in the saphenous vein at the ankle in man during exercise and changes in posture. Journal of applied physiology 1, 649-662.

Rachev, A., Greenwald, S.E., 2002. Residual strains in conduit arteries. Journal of Biomechanics 36, 661-670.

Sassani, S. G., Theofani, A., Tsangaris, S., Sokolis, D. P., 2013. Time-course of venous wall biomechanical adaptation in pressure and flow-overload: Assessment by a microstructure-based material model. Journal of Biomechanics 46, 2451-2462.

Sokolis, D. P., 2013. Experimental investigation and constitutive modeling of the 3D histomechanical properties of vein tissue. Biomechanics and Modeling in Mechanobiology 12, 431-451.

Stooker, W., Gök, M., Sipkema, P., Niessen, H.W.M., Baidoshvili, A., Westerhof, N., Jansen, E.K., Wildevuur, C.R.H., Eijsman, L. , 2003. Pressure-Diameter Relationship in the Human Greater Saphenous Vein. Annals of Thoracic Surgery 76, 1533-1538.

Takamizawa, K., Hayashi, K., 1987. Strain energy density function and uniform strain hypothesis for arterial mechanics. Journal of Biomechanics 20, 7-17.

Tran-Son-Tay, R., Hwang, M., Garbey, M., Jiang, Z., Ozaki, C. K., Berceli, S. A., 2008. An experiment-based model of vein graft remodeling induced by shear stress. Annals of Biomedical Engineering 36, 1083-1091.

Wesly, R.L.R., Vaishnav, R.N., Fuchs et, a.J.C.A., Patel, D.J., Greenfield Jr., J.C., 1975. Static linear and nonlinear elastic properties of normal and arterialized venous tissue in dog and man. Circulation Research 37, 509-520.

Zhao, J., Jesper Andreasen, J., Yang, J., Steen Rasmussen, B., Liao, D., Gregersen, H., 2007. Manual pressure distension of the human saphenous vein changes its biomechanical properties - implications for coronary artery bypass grafting. Journal of Biomechanics 40, 2268-2276.

List of Selected Publications

Papers Related to the Thesis

- **Journal papers**

  Horny, L., Adamek, T., Vesely, J., et al., 2012. Age-related distribution of longitudinal pre-strain in abdominal aorta with emphasis on forensic. Forensic Science International 214, 18-22. **IF 1.95 – 11 citations in Scopus**

  Veselý, J., Horný, L., Chlup, H., Adámek, T., Krajíček, M., Žitný, R., 2015. Constitutive modeling of human saphenous veins at overloading pressures. Journal of the Mechanical Behavior of Biomedical Materials 45, 101–108. 5-year **IF 3.152 – 4 citations in Scopus**

- **Conference papers**

  Vesely, J., Horny, L., Chlup, H., Adamek, T., & Zitny, R., 2015. Opening angle of human saphenous vein. In: *Proceedings of the 8th International Conference on Computational Plasticity - Fundamentals and Applications, COMPLAS 2015*, 457-462.

  Veselý, J., Horný, L., Chlup, H., Krajíček, M., Žitný, R., 2015c. The Influence of the Opening Angle on the Stress Distribution through the Saphenous Vein Wall. In: *IFMBE Proceedings of 6th European Conference of the International Federation for Medical and Biological Engineering, MBEC 2014; Dubrovnik; Croatia*, 399-402.

  Veselý, J., Horný, L., Chlup, H., Žitný, R., 2014. Inflation Tests of Vena Saphena Mangna for Different Loading Rates. In: *IFMBE Proceedings of 13th Mediterranean Conference on Medical and Biological Engineering and Computing 2013, MEDICON 2013; Seville; Spain*, 1041-1044.

  Vesely, J., Hadraba, D., Chlup, H., Horny, L., Adamek, T., & Zitny, R., 2014. Constitutive modelling and histology of vena saphena doi:10.4028/www.scientific.net/AMM.486.249

Other publications

- **Journal papers**

  Suchý, T., Šupová, M., Klapková, E. et al., 2016. The sustainable release of Vancomycin and its degradation products from nanostructured collagen/hydroxyapatite composite layers. Journal of Pharmaceutical Sciences 105, 1288-1294**. IF 2.59 – 1 citation in Scopus**

  Veselý, J., Horný, L., Chlup, H. et al., 2015. Effect of Polyvinyl Alcohol Concentration on the Mechanical Properties of Collagen/Polyvinyl Alcohol Blends [online]. *Applied Mechanics and Materials* 732, 161-164.

  Horny, L., Chlup, H., Zitny, R., et al., 2012. Ex Vivo Coronary Stent Implantation Evaluated with Digital Image Correlation. Experimental Mechanics 52, 1555-1558. **IF 1.764 – 2 citations in Scopus**

- **Conference papers**

  Veselý, J., Chlup, H., Krajíček, M., et al., 2015. Mechanical properties of biological composite reinforced by polyester mesh. In: *Experimental Stress Analysis 2015. Experimentální analýza napětí 2015; Český Krumlov; Czech Republic*, 466-468.

  Vesely, J., Horny, L., Chlup, H., et al., 2014. Mechanical properties of polyvinyl alcohol/collagen hydrogel. In: *52nd International Conference on Experimental Stress Analysis, EAN 2014; Marianske Lazne; Czech Republic*.

  Veselý, J., Horný, L., Gultová, E., et al., 2012. The deformation analyses of an elastomeric composite reinforced by superelastic wires. In: *50th Annual Conference on Experimental Stress Analysis, EAN 2012; Tabor; Czech Republic* – **1 citation in Scopus**